Progress In Electromagnetics Research B, Vol. 23, 147–164, 2010

THEORETICAL COMPARATIVE STUDIES OF CROSS-SECTION EVALUATION IN ERBIUM-DOPED OPTICAL FIBERS

M. Karimi

Physics Group
Razi University
Kermanshah, Iran

F. E. Seraji

Optical Communication Group
Iran Telecom Research Center
Tehran 14399, Iran

Abstract—In this paper, we introduce a different approach of previously reported method to determine absorption and emission cross-sections (σ_a and σ_e), and dopant concentration in Erbium doped optical fibers (EDOFs) with low background loss (α). We call this new method as variant input single cutback method (VISCM). There is technical similarity between VISCM and conventional cutback method (CCM) for determination of cross-sections, but in former pump and signal powers are not used together. We numerically verify the effect of different parameters such as input power, background loss, and EDOF amplifier cutback length on the cross-sections using VISCM and CCM. We also present the simulation results of maximum gain and optimum length using obtained cross-sections by two methods. We show that the VISCM presents more accuracy than that of CCM in any conditions. In the presence of α, both CCM and VISCM give not actual but pseudo values for the σ_a and σ_e. Using pseudo parameters values obtained by VISCM for $\alpha < 10\,\mathrm{dB/km}$, the error of maximum gain and optimum length of designed EDOF is shown negligible.

Received 23 May 2010, Accepted 8 July 2010, Scheduled 21 July 2010
Corresponding author: F. E. Seraji (feseraji@itrc.ac.ir).

1. INTRODUCTION

There are several devices based on Erbium doped optical fibers (EDOFs) such as optical sensors [1], lasers, and optical amplifiers [2, 3]. To design and improve such devices, we need to know the main parameters of EDOFs. Absorption and emission cross-sections [4], dopant concentration and distribution in the fiber core, background loss (α), and steady-state lifetime are the main parameters of the EDOFs. The main technique for measurements of the σ_a and σ_e without co-dopants can be performed by a theoretical method called as Judd-Ofelt [5–7] that is based on atomic level structure. Using Fuchtbauer-Ladenburg equations enables us to evaluate experimentally the steady-state lifetime of the EDOFs, which is an accurate but costly method [2, 8, 9]. Conventional cutback method (CCM), which is a simple and low cost technique, can be also used to evaluate the σ_a and σ_e of the EDOFs [2, 10, 11]. Dopant concentration can be determined using small angle X-ray scattering study [12], scanning electron microscopy or X-ray diffraction methods [13]. The value of α can be measured by the step function method [14], CCM [2] and Zech technique [15–17].

Recently, we have reported experimental techniques for simultaneous measurement of the σ_a, σ_e and α in lossy DOFs [18–20] and low-loss ($< 10\,\mathrm{dB/km}$) EDOF [21]. In the present paper, with an aim of theoretical comparative studies of our proposed technique and the CCM, we will utilize the same method but with a different approach to evaluate simultaneously the σ_a, σ_e and dopant concentration in low-loss EDOFs, which is based on variant input power, hence the name variant input single cutback method (VISCM). The advantage of implementing our model is that the pump power is not required, as σ_a and σ_e are almost obtainable with a mono-beam operation of the EDOF at any wavelength. But to evaluate σ_a and σ_e by CCM, the pump power must be used. In our comparative studies, we choose a low-loss DOF such as Erbium DOF and show that our model has more accuracy than CCM in evaluating σ_a, σ_e, and the gain of an EDOF. In addition, the analysis show that our model has a good agreement with the actual values of the maximum gain and optimum length of the EDOF with α less than about $10\,\mathrm{dB/km}$.

Moreover, while using our model to characterize an EDOF with a low value of α, contrary to CCM, we need not to determine α of the sample, which in turn makes the rate equations simple. The proposed characterization models are simple and low cost that can have an advantageous use in measuring tasks of the EDOF characteristics in manufacturing process. We note that both methods VISCM and CCM do not give actual values of the EDOF parameters.

2. CROSS-SECTIONS MODELS USING CCM AND VISCM

In our previous report using VISCM [21], a mono-beam propagation was used for determination of cross-sections in a low loss EDOF, but in using CCM, a double-beam propagation is used for the same purpose. The models of σ_a, σ_e, and the dopant concentration (N_t) using VISCM were obtained as [21]:

$$\sigma_a = \frac{\ln\frac{P_{21}}{P_{11}}(P_{22}-P_{12}) - \ln\frac{P_{22}}{P_{12}}(P_{21}-P_{11})}{L\,N_t\,\Gamma\,(P_{22}-P_{12}-P_{21}+P_{11})} \quad (1)$$

$$\sigma_e = \frac{\pi r^2 (h\nu/\tau)}{\Gamma}\,\frac{\ln\frac{P_{21}}{P_{11}} - \ln\frac{P_{22}}{P_{12}}}{(P_{22}-P_{12}-P_{21}+P_{11})} - \frac{1}{L\,N_t\,\Gamma}\,\frac{\ln\frac{P_{21}}{P_{11}}(P_{22}-P_{12}) - \ln\frac{P_{22}}{P_{12}}(P_{21}-P_{11})}{(P_{22}-P_{12}-P_{21}+P_{11})} \quad (2)$$

$$N_t = \frac{1}{L\cdot\pi r^2\cdot(h\nu/\tau)}\cdot\frac{\ln\frac{P_{21}}{P_{11}}(P_{22}-P_{12}) - \ln\frac{P_{22}}{P_{12}}(P_{21}-P_{11})}{\ln\frac{P_{21}}{P_{11}} - \ln\frac{P_{22}}{P_{12}}} \quad (3)$$

where P_{11}, P_{12} and P_{21}, P_{22} are the measured output powers of EDOF for full length and cutback length, respectively, for input powers varied twice, using Figure 3 in Ref. [21].

We note that for measuring N_t, the input signal should be at 980 nm.

For determination of cross-sections using CCM, the pump is turned on and the output power is measured as P_{p1}, then the pump is turned off and corresponding power at the same point is measured as P_{s1}. In the second step, a small fiber length L is cutback and the signal powers are measured as P_{p2} and P_{s2} when the pump is on and off, respectively.

In a single mode EDOF, assuming unsaturated condition and the negligible value of α, the value of σ_e is obtained at high pump regime and σ_a is obtained from signal loss coefficient (α_l) in the absence of pumping as follow [3]:

$$\sigma_e(\lambda_s) = \frac{g_s}{N_t\,\Gamma} = \frac{\log(P_{p1}/P_{p2})}{N_t\,L} \tag{4}$$

$$\sigma_a(\lambda_s) = \frac{\alpha_\ell}{N_t\,\Gamma} = -\frac{\log(P_{s1}/P_{s2})}{N_t\,L} \tag{5}$$

where $\Gamma = 1 - \exp(-2R^2/\omega^2)$ is overlap factor of a step index single-mode fiber (SMF) [22], where R is radius of constant Erbium distribution in the core of the DOF, which is approximated to core radius (r), and ω is the spot size, which is defined as a function of V-parameter of the fiber as $\omega = r\,(0.65 + 1.619/V^{1.5} + 2.879/V^6)$ [23]. The value of Γ factor for the SMF is nearly unity.

3. SIMULATION RESULTS AND DISCUSSIONS

For theoretical determination of σ_a and σ_e values in a lossless EDOF at a given wavelength, we must extract the output responses using formulation of each method. In the present paper, we choose an Al/P/Er-DOF as a sample for comparative characterizations using VISCM, CCM, and Fuchtbauer-Ladenburg (FL) approach. Our intention in the comparative studies of the sample is to show that the results obtained by VISCM and CCM are not actual values rather pseudo ones whereas the results pertaining to FL approach [4] would be actual measured values. We remind that α term is not included in the FL approach, hence the reason of referring the results of FL approach as actual ones is justified in our analysis. Finally, we will show that the pseudo values of our proposed method VISCM are closer to the actual values than that of CCM.

In VISCM for the sample Al/P/Er-DOF, we take input powers of 4 and 7 mW at lengths $Z_0 = 0.9$ m and $Z_1 = 0.4$ m to simulate the output powers, using Eq. (4) at given wavelengths. By using results of Eqs. (1) and (2), the values of σ_a and σ_e in the lossless sample are obtained and depicted in Figure 1. As shown in this figure, the obtained values of cross-sections are the same as the actual values of FL approach, as we expected, because we used exact form of mono-beam propagation [15, 24]. The required parameters for the simulation are selected from Table 1.

To simulate the results of CCM in a similar condition as above, the rate equations [21, 25] are solved by Runge-Kutta method [26] with signal and pump powers assumed as 4 mW and 50 mW, respectively. The obtained results are used in Eqs. (4) and (5) to simulate σ_a and σ_e of the sample, assuming $\lambda_p = 980$ nm, as illustrated in Figure 1. As it is shown in this case, the values of cross-sections obtained by CCM are

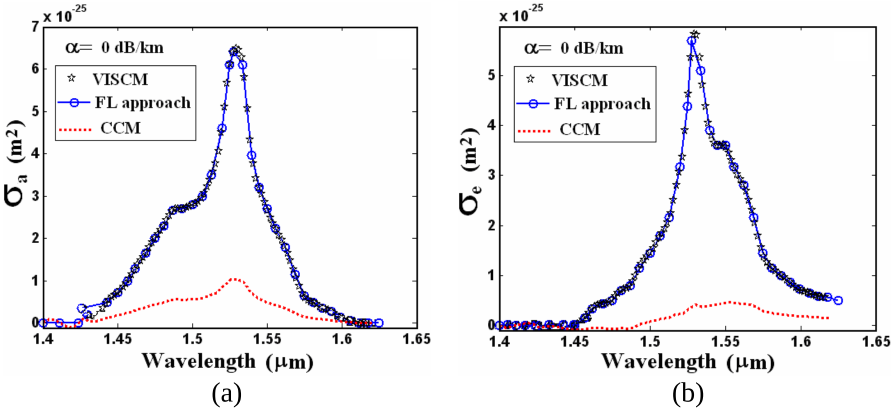

Figure 1. Simulated values of (a) σ_a and (b) σ_e of lossless Al/P/Er DOF using VISCM and CCM. The actual values of the σ_a and the σ_e are indicated by FL approach.

lower than the actual values obtained by FL approach in the lossless condition whereas the results obtained by VISCM coincide with the actual curve, hence more accuracy resulted by VISCM.

As mentioned previously, the cross-sections are obtained using Eqs. (1), (2) based on a lossless EDOF, which was extracted from mono-beam equation. Since in practice, a lossless EDOF does not really exist, then for simulation we should insert α term in propagation relation to evaluate its effect on the output powers for final assessments of the cross-sections using Eqs. (1), (2).

Therefore, the output power variations versus the length of a lossy EDOF is [15, 24]:

$$\frac{\partial P}{\partial z} = -\alpha_{er} \frac{1}{1 + P/P_{sat}} P - \alpha P \tag{6}$$

where α_{er} is the Erbium absorption coefficient. Eq. (6) has analytical

Table 1. Parameters values for simulation of Al/P/Er-DOF.

Al/P/Er-DOF Parameters [4]		
$\lambda_p = 980\,\text{nm}$	$\lambda_s = 1530\,\text{nm}$	$\lambda_s = 1550\,\text{nm}$
$\sigma_a^p = 5.6 \times 10^{-25}\,\text{m}^2$	$\sigma_a^s = 6.5 \times 10^{-25}\,\text{m}^2$	$\sigma_a^s = 2.7 \times 10^{-25}\,\text{m}^2$
	$\sigma_e^s = 5.9 \times 10^{-25}\,\text{m}^2$	$\sigma_e^s = 3.6 \times 10^{-25}\,\text{m}^2$
$r = 2.6\,\mu\text{m}$; $\tau = 10\,\text{ms}$; $N_t = 10^{25}\,\text{ion/m}^3$		

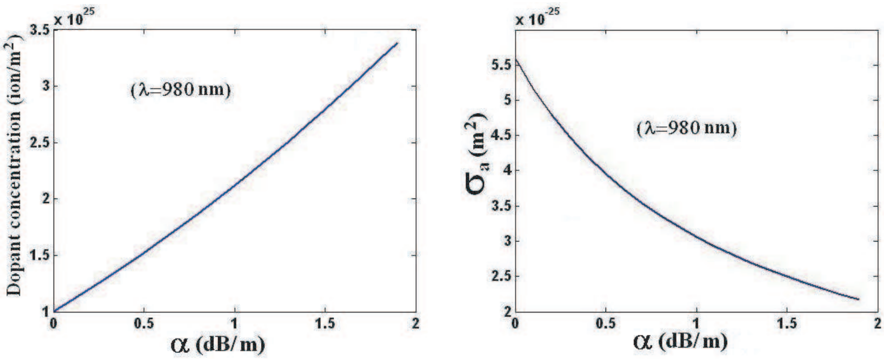

(a) (b)

Figure 2. (a) The pseudo dopant concentration, (b) the pseudo σ_a variations of Al/P/Er DOF using VISCM.

solution [15], but in this paper we solve it by Runge-Kutta method [26] at a given wavelength. By using 980 nm as input wavelength, the variations of output power at the same lengths $Z_0 = 0.9\,\mathrm{m}$ and $Z_1 = 0.4\,\mathrm{m}$ (as in Figure 1) for input power of 4 and 7 mw for different values of α are determined. The determined output powers are utilized in Eqs. (1), (2) and (3) to evaluate the variations of σ_a at 980 nm and dopant concentration in a lossy EDOF. When α in EDOF increases, the σ_a value will decrease linearly whereas the dopant concentration is increased, as shown in Figure 2.

It is noted that by including α in the mono-beam equation (Eq. (6)), the effect of the loss reflects itself in the obtained values in Figure 2, resulting in no actual values for the σ_a and the dopant concentration.

To differentiate the parameters values obtained from Eq. (6) and mono-beam relation, for lossy and lossless conditions, respectively, we term the results from Eq. (6) as pseudo parameters values, i.e, pseudo cross-sections and pseudo dopant concentration. Here, as in cases of Eqs. (1)–(3), by the prefix *pseudo* we mean not *actual*.

By solving Eq. (6) at a given wavelength and then using Eqs. (1) and (2) the values of σ_a and σ_e are determined. In Eqs. (1) and (2), we can replace the dopant concentration either by its actual or pseudo value. For actual and pseudo values of dopant concentrations, the corresponding variations of σ_a and σ_e are depicted in Figure 3 at 1550 nm and 1530 nm. In addition, by inserting a value for α in rate equations [21, 25], the variations of signal power in presence of α is obtained. Now, based on CCM procedure for determination of σ_a and

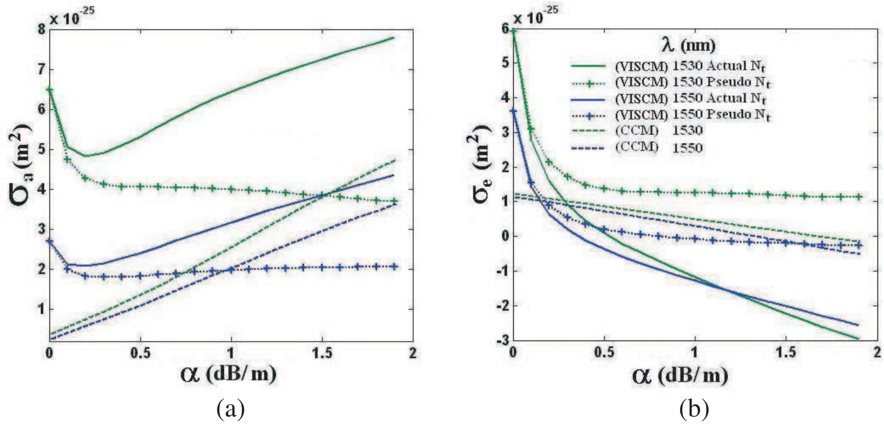

Figure 3. Variations of (a) pseudo σ_a and (b) pseudo σ_e as functions of α in Al/P/Er DOF at 1530 and 1550 nm using VISCM and CCM with pseudo and actual dopant concentrations.

σ_e, the values of the pseudo σ_a and the pseudo σ_e at 1550 and 1530 nm in presence of α are obtained from Eqs. (4), (5) and are shown in the same Figure 3.

As observed in Figure 3(a), using VISCM at 1530 nm and 1550 nm, the pseudo values of σ_a for actual and pseudo values of N_t monotonically decrease to minimum values when $\alpha = 0.19$ dB/m and $\alpha = 0.13$ dB/m, respectively, and then increases for actual N_t, while almost remain constant for pseudo N_t. For the higher α, by using actual N_t (solid curve), the value of pseudo σ_a at 1530 nm is the same as actual one at $\alpha = 1.03$ dB/m whereas at 1550 nm the value of pseudo σ_a equals actual one at $\alpha = 0.75$ dB/m.

As shown in Figure 3(b), as α increases, the pseudo values of σ_e decrease using actual N_t, while using pseudo N_t, the pseudo values of σ_e tends to a constant value. When using actual value of N_t, the pseudo values of σ_e are less than the case of using pseudo value of N_t. Using actual N_t in VISCM to determine pseudo σ_e at 1530 and 1550 nm for α greater than 0.55 and 0.36 dB/m, respectively, the values of pseudo σ_e become negative, as shown in Figure 3(b), indicating that this method is only valid for $\alpha < 0.36$ dB/m.

We note in Figure 3, when α increases, using actual value of N_t would give high error in determination of the cross-sections, where in case of pseudo σ_e, the error is more. So in comparison of using pseudo and actual N_t to determine pseudo cross-section, the pseudo value of N_t is preferred.

Using CCM to determine the cross-sections, by increasing α in the sample, the value of the pseudo σ_a increases while the value of the pseudo σ_e decreases, as noted in Figure 3. In a comparison of VISCM with CCM, at the lower values of α, the VISCM shows that the pseudo values of the cross-sections are more closer to actual ones than in case of the CCM. At the higher values of α, the two methods have results of nearly equal errors. So at high α, the two methods have no superiority on each other. The actual values of σ_a and σ_e at 1530 and 1550 nm are presented in Table 1.

In CCM, not only the presence of α in the sample affects on the pseudo values of cross-sections but also other input variables such as input signal power would affect on the parameters values. For example, when the input signal power increases, the pseudo value of σ_a and σ_e will change and go farther than actual ones, as illustrated in Figure 4. Therefore, in practice, the value of input signal power must be very low to increase the accuracy of experiment when using CCM.

The effect of input pump power, on the result of CCM determination of σ_e with $\alpha = 10\,\text{dB/km}$ is shown in Figure 5. The value of σ_e will increase up to the actual value when the pump power increases as compared with data in Table 1. Therefore, in a practical case, for a high value of the pump power, the value of σ_e will be closer to its actual value. It is noted that for determination of the σ_a using CCM, the pump power is turned off, hence no effect of pump power is envisaged on the σ_a.

Variations of σ_a and σ_e with respect to input signal power change

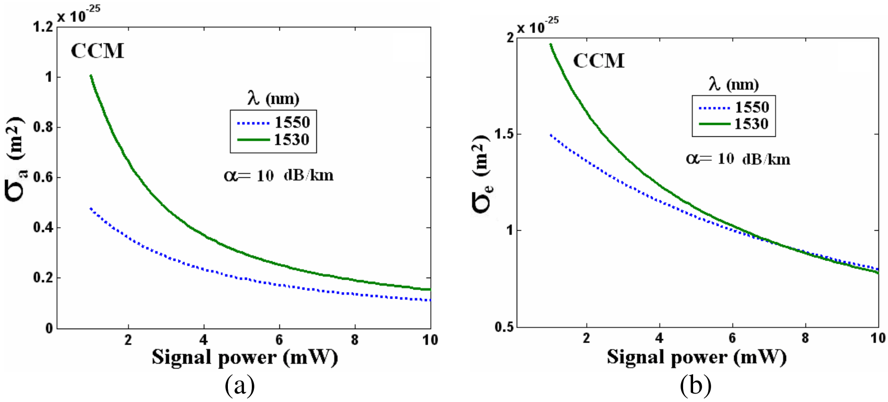

Figure 4. Variations of (a) pseudo σ_a and (b) pseudo σ_e as a function of input signal power in Al/P/Er DOF at 1530 and 1550 nm using CCM.

ΔP using VISCM are depicted in Figure 6 at two wavelengths for actual and pseudo dopant concentrations, where $\Delta P = P_{in2} - P_{in1}$. We note that when using VISCM, the values of σ_a and σ_e are not affected by input signal power as compared with CCM.

Another influential factor on results of both the measuring methods is the EDOF cutback length. The variation of output results of VISCM by increasing EDOF cutback length are shown in Figure 7 at 1550 and 1530 nm for a lossy EDOF. As observed from Figures 7(a), 7(b), 7(c), by increasing the EDOF cutback length, the pseudo pump $\sigma_a(=\sigma_a^p)$, pseudo signal $\sigma_a(=\sigma_a^s)$ and the pseudo signal $\sigma_e(=\sigma_e^s)$ tend

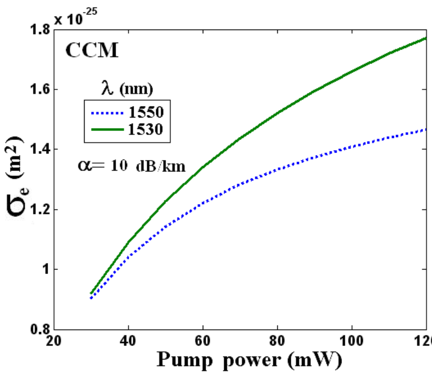

Figure 5. Variation of the pseudo σ_e as a function of pump power in Al/P/Er DOF at 1530 and 1550 nm using CCM.

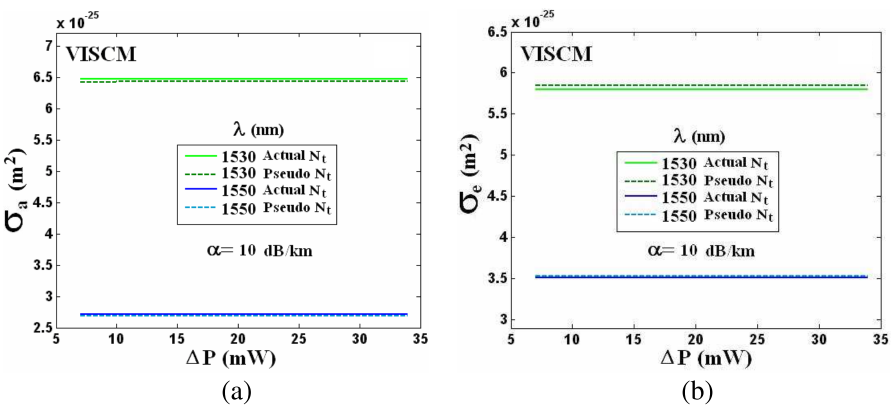

Figure 6. Variations of (a) the pseudo σ_a and (b) the pseudo σ_e as a function of input signal power change in Al/P/Er DOF at 1530 and 1550 nm using VISCM with actual and pseudo dopant density.

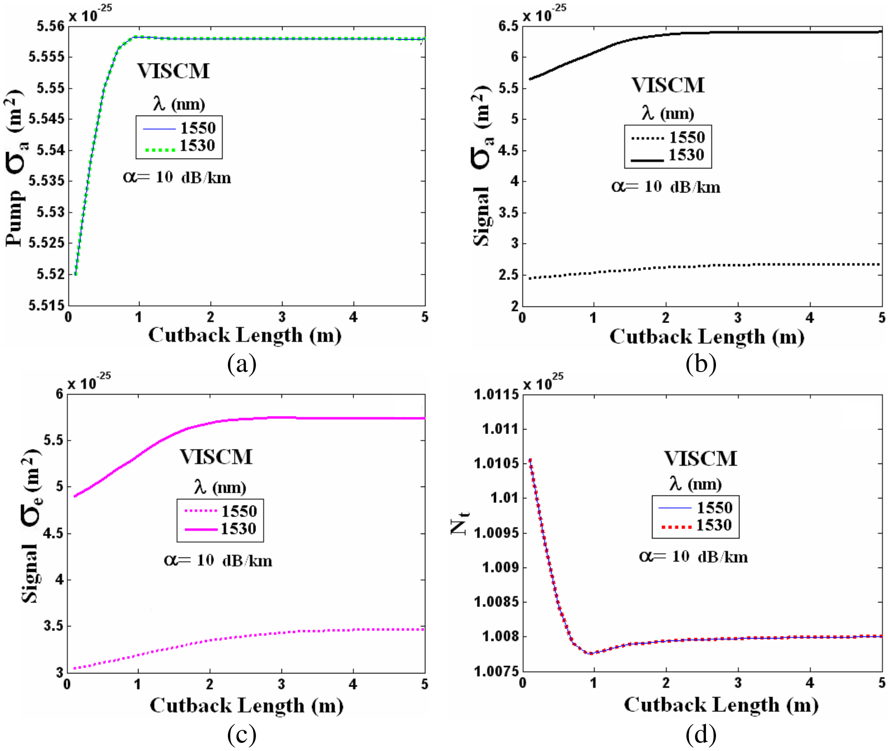

Figure 7. Variations of pseudo (a) pump σ_a, (b) signal σ_a, (c) signal σ_e, and (d) dopant concentration with respect to EDOF cutback length using VISCM. Input wavelength = 1550 nm and 1530 nm and $\alpha = 10\,\mathrm{dB/km}$, input power = 4 mW.

to constant values, approaching the actual ones at cutback length of 1 m, 2 m, and 2 m, respectively. So in using input power of 4 mW, the best EDOF length for cutback is about 2 m. In Figure 7(d), dopant concentration approaches to a constant value for EDOF cutback length of about 1 m.

Similar to Figure 7, the effect of EDOF cutback length for CCM is also simulated, as illustrated in Figure 8. As observed in Figures 8(a), 8(b), by increasing the cutback length the pseudo values of the σ_a at pump and signal wavelengths are increased while the pseudo value of σ_e at signal wavelength is decreased, as shown in Figure 8(c). By increasing the EDOF cutback length, the pseudo values of σ_a improve to the actual values whereas the pseudo value of σ_e keeps away from it. So deciding to introduce a proper EDOF cutback length is not straight forward in CCM, because for σ_e short cutback length and for the σ_a longer cutback length is suitable to obtain actual values.

Now we want to see that how different are the pseudo gain and the optimized length of the EDOF, obtained from pseudo cross-sections by VISCM, CCM, and the corresponding results yielded by FL approach. To illustrate the actual gain, we assume α is practically present and the rate equations are solved for the cross-sections which are resulted from FL approach. However, we noted previously that α in the formulations of VISCM and CCM was not considered, but in practice its presence would affect the cross-sections. Similarly, for determination of pseudo gain by VISCM and CCM, the rate equations are solved without α using pseudo cross-sections. Moreover, we note that in VISCM, pseudo concentration is used instead of the actual one.

Using the actual- and pseudo-values of σ_a^s, σ_a^p and σ_e^s from Figure 3 at $\lambda_s = 1550\,\text{nm}$ and $\lambda_p = 980\,\text{nm}$, respectively, and the corresponding dopant concentrations, the actual- and pseudo-values of the gain are obtained in terms of EDOF length for different values of α. The results of the simulation for VISCM and CCM are plotted in Figures 9(a) and 9(b), respectively.

Here, for the plot of pseudo gain of CCM, first by using rate equations [21, 25], the value of σ_a at 980 nm is obtained when only pump is on. In other word we use 980 nm as signal wavelength. In this simulation, we have taken actual $N_t = 1 \times 10^{25}\,\text{ion/m}^3$, $\tau = 10\,\text{ms}$, and $\alpha_s = \alpha_p = \alpha$ (Variant). Like in previous cases, in our analysis, we have called all the gains obtained from any techniques as pseudo gains, which differ from actual ones.

In Figure 9(a), the values of pseudo gains obtained from VISCM are close to actual ones as compared with Figure 9(b), which is determined from CCM. As shown in Figure 9(b), for any α values (i.e., $\alpha = 10$, 50, 100 dB/km), the pseudo gain becomes about 15 dB lower than that of actual ones. But in Figure 9(a) using VISCM the pseudo gain shows lower error than that of CCM. So use of CCM to measure σ_a and σ_e is not recommended, because of high error in the gain.

More investigations are carried out on the effect of α of EDOF on the maximum differences between the actual and pseudo gain values given by $\Delta G_{\text{max}} = G_{\text{max}}(\text{pseudo}) - G_{\text{max}}(\text{actual})$ and the corresponding difference in the optimized EDOF length expressed as $\Delta L_{\text{opt}} = L_{\text{opt}}(\text{pseudo}) - L_{\text{opt}}(\text{actual})$. The results of VISCM are illustrated in Figures 10(a) and 10(b) for two signal wavelengths 1530 nm and 1550 nm, respectively.

When α of EDOF increases, the maximum difference between the actual- and pseudo- gain values and the corresponding difference in the

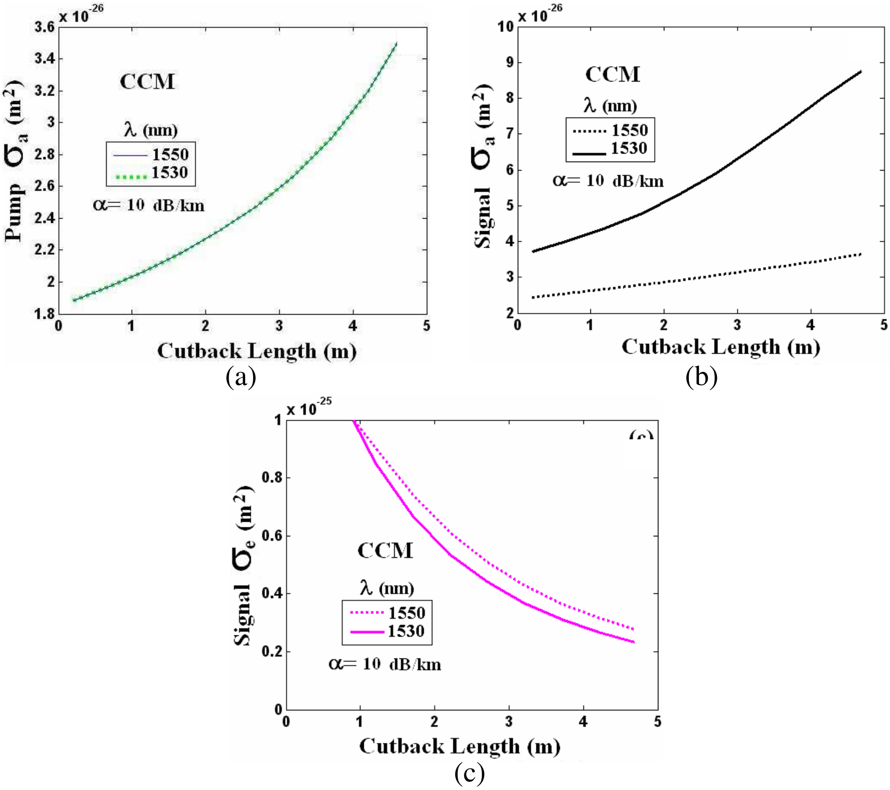

Figure 8. Variations of pseudo (a) σ_a^p, (b) σ_a^s, (c) σ_e^s with respect to EDOF cutback length using CCM. Input wavelengths = 1550 nm and 1530 nm and $\alpha = 10\,\mathrm{dB/km}$, the pump power = 50 mW and signal power = 4 mW.

optimized EDOF lengths ΔL_{opt} will increase. The difference $\Delta G_{\max}$ and ΔL_{opt} for shorter signal wavelength are higher. For instance, at $\alpha = 80\,\mathrm{dB/km}$, and 1550 nm, $\Delta G_{\max}$ is about 0.9 dB and ΔL_{opt} is 1.2 m long while at 1530 nm they are 1.2 dB and 1.6 m, respectively.

Similarly, the variations of $\Delta G_{\max}$ and ΔL_{opt} with respect to α using CCM, are depicted in Figure 11 for both 1550 nm and 1530 nm. As shown in Figure 11(a), the effect of α growth on $\Delta G_{\max}$ beyond about 10 dB/km is almost constant. We note that the use of the cross-sections obtained by CCM to design amplifier, creates about 10 dB/km error in determination of gain, and the value of optimum length is more than 7 m longer than the actual one.

In Table 2, the calculated error % of maximum gain

($\Delta G_{\max}/G_{\max}$(actual) $\times$ 100) and error % of the optimum length ($\Delta L_{\mathrm{opt}}/L_{\mathrm{opt}}$(actual) $\times$ 100) of EDOF using VISCM and CCM are compared. It is observed from Figure 9(a) that for α up to 10 dB/km, the differences between the actual and pseudo gain values are negligible. However, when α in the EDOF amplifier increases, the pseudo gain value becomes less than the actual value.

In most recent EDOFs in the market, α value is limited to 10 dB/km [27, 28]. At this α value, the maximum difference between the actual and pseudo gain values is about 0.2 dB, as shown in Figure 10 for VISCM, and the optimized length difference of the EDOF amplifier

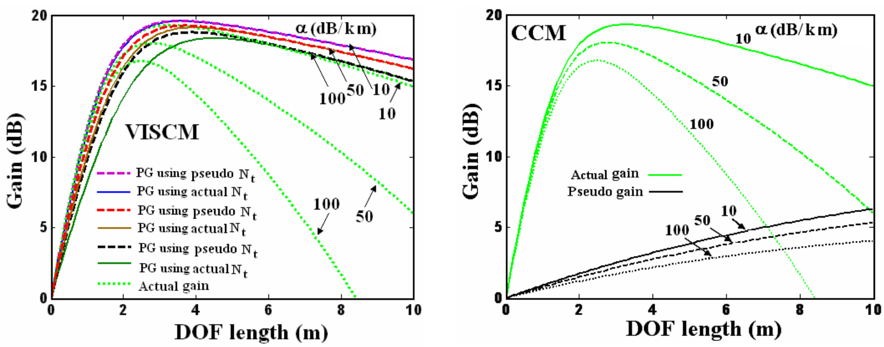

(a) (b)

Figure 9. Variations of pseudo- and actual gains of Al/P/Er DOF amplifier for different values of α using (a) VISCM, (b) CCM. PG stands for pseudo gain.

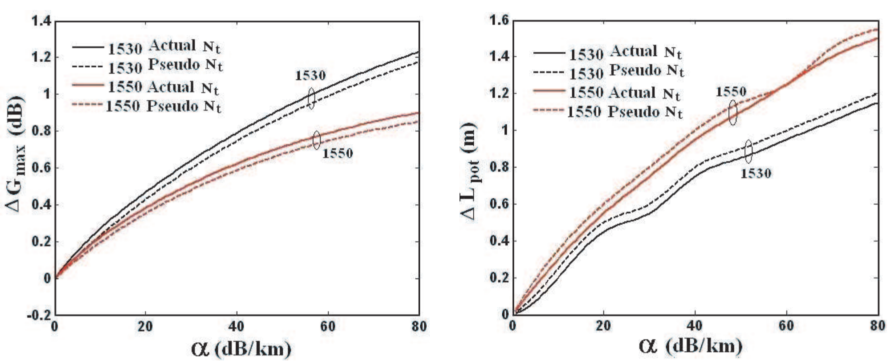

(a) (b)

Figure 10. (a) Maximum difference between actual and pseudo gain values and (b) corresponding optimized EDOF length at 1530 and 1550 nm using VISCM.

Table 2. Comparison of calculated error % of VISCM and CCM.

Max. gain/Opt. length	Error % at 10 dB/km		
	VISCM with:		CCM
	Actual N_t	Pseudo N_t	
Max. gain at 1550 nm	1.49%	1.62%	67.40%
Max. gain at 1530 nm	1.40%	1.57%	73.31%
Optimum length At 1550 nm	9%	9%	$> 200\%$
Optimum length At 1530 nm	10%	10%	$> 230\%$

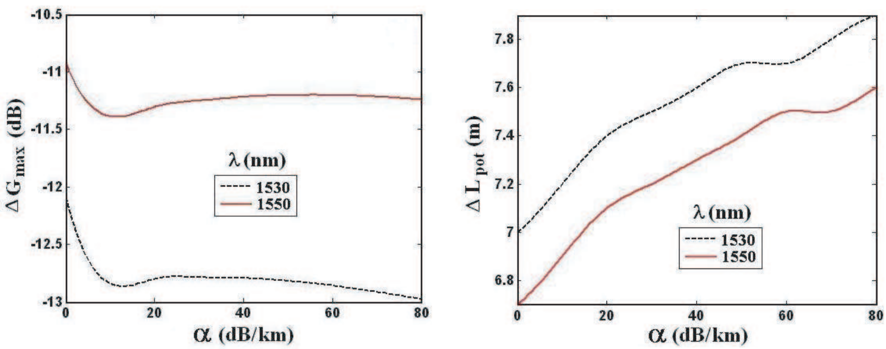

(a) (b)

Figure 11. (a) Maximum difference between actual and pseudo gain values and (b) corresponding optimized EDOF length difference at 1530 and 1550 nm using CCM.

between actual and pseudo-values is quite negligible (i.e., 0.2 m). Therefore, for characterization of a low-α EDOFs, pseudo parameter values can be useful using VISCM.

In using the proposed method (VISCM)) for characterization of an Al/P/Er DOF with a low-α, not only the parameters are determined simultaneously but also there is no need of considering α in design procedure of optical amplifier. In VISCM, although at the preliminary stage pseudo parameter values are assumed for simulation, the outcome of the calculation yields a relatively accurate optimized EDOF length for a maximum gain value.

The results of the analysis are summarized in Table 3 where the proposed method is compared with our former work and the method CCM and FL approach.

Table 3. Comparison of the proposed method with others.

Methods	VISCM		Our former work [18, 19]	CCM	FL
	Actual N_t	Pseudo N_t			
Measurands	σ_a, σ_e, N_t	σ_a, σ_e	σ_a, σ_e, α, N_t	σ_a, σ_e	σ_a, σ_e
Measurable range of loss	-Valid for low loss with accuracy higher than CCM -For high loss, accuracy similar to CCM	-Valid for low loss with higher accuracy than CCM -For high loss accuracy lower than CCM	No limitation	Valid for high loss	No limitation
Type of parameters	Pseudo	Pseudo	Actual	Pseudo	Actual
Accuracy	Medium	Medium	High	Medium	Higher
Range of Cutback length	2 m	2 m	No range*	Not determi- nistic*	No range
Range of input power	No limitation	No limitation	No limitation	High	No limitation

*To avoid ASE effect, the cutback length should be less than 2 m.

4. CONCLUSION

This paper presents a simple novel method to characterize Erbium doped optical fibers with low background losses of less than 10 dB/km. The absorption- and emission cross-sections, and dopant concentration can simultaneously be determined by this method.

In the new technique, called as variant input single cutback method (VISCM), the input power is varied twice, and the corresponding powers (intensities) at initial and cutback length are measured.

For a comparison with VISCM, we have reviewed the conventional cutback method (CCM) for determination of emission- and absorption cross-sections, and verified the effect of pump and signal powers on the results of cross-sections values using CCM. The results of analysis of both the methods are compared with Fuchtbauer-Ladenburg approach. We have shown that our new model is not sensitive to input power values whereas in CCM, when the input pump power is low and/or the signal power is high, the values of cross-sections and the gain show relatively high errors.

The effect of existing background loss in EDOF on the results of VISCM and CCM are analyzed. Our new model exhibits lower sensitivity to background loss as compared with CCM.

In both methods the results depend on the EDOF cutback length. We have shown in our model the best EDOF cutback length is about 2 m. On the other hand, the CCM has more sensitivity to EDOF cutback length.

The parameters values, obtained by both methods, are assumed to be pseudo values rather actual ones that is obtained by Fuchtbauer-Ladenburg approach

The simulations show that for Erbium doped glass fibers with background loss less than 10 dB/km, the difference between the maximum gains and optimum length obtained with pseudo- and the actual values are negligible.

REFERENCES

1. Zhang, Y., M. Zhang, W. Jin, H. L. Ho, M. S. Demokan, X. H. Fang, B. Culshaw, and G. Stewart, "Investigation of erbium-doped fiber laser intra-cavity absorption sensor for gas detection," *Opt. Commun.*, Vol. 232, 295–301, 2004.
2. Harun, S. W., X. S. Cheng, N. K. Saat, and H. Ahmad, "S-band Brillouin erbium fibre laser," *Electron. Lett.*, Vol. 41, 174–176, 2005.
3. Desurvire, E., *Erbium Doped Fiber Amplifiers: Principles and Applications*, Wiley, New York, 1994.
4. Barnes, W. L., R. I. Laming, E. J. Tarbox, and P. R. Morkel, "Absorption and emission cross sections of Er^{3+} doped silica fibers," *IEEE. J. Quant. Electron.*, Vol. 27, 1004–1010, 1991.
5. Walsh, B., *Judd-Ofelt Theory: Principles and Practices, Advances in Spectroscopy for Lasers and Sensing*, Vol. 33, 403–433, Springer, The Netherlands, 2006.
6. Lin, H., G. Meredith, S. Jiang, X. Peng, T. Luo, and N. Peyghambarian, "Optical transitions and visible upconversion

in Er^{3+} doped niobic tellurite glass," *J. Appl. Phys.*, Vol. 93, 186–191, 2003.

7. Jianhu, Z., J. Yang, and S. Dai, "Optical Spectroscopy and gain properties of Nd^{+3} doped oxide glasses," *J. Opt. Soc. Am. B*, Vol. 21, 739–743, 2004.
8. Mahran, O., "Yttria-alumina-silicate erbium doped fiber amplifier characteristics at 1540 nm," *Int. J. Pure Appl. Phys.*, Vol. 3, 83–90, 2007.
9. Liu, G. and B. Jacquier, *Spectroscopic Property of Rare Earths in Optical Materials*, Springer, Heidelberg, Germany, 2005.
10. Giles, C. R. and D. Digiovanni, "Spectral dependence of gain and noise in erbium-doped fiber amplifiers," *IEEE, Photon. Technol. Lett.*, Vol. 2, 797–800, 1990.
11. Giles, C. R., C. A. Bums, D. J. DiGiovanni, N. K. Dutta, and G. Raybon, "Characterization of erbium-doped fibers and application to modeling 980-nm and 1480-nm pumped amplifiers," *IEEE Photon. Technol. Lett.*, Vol. 3, 363–365, 1991.
12. Martinez, V., A. M. Jurdyc, D. Vouagner, C. Martinet, and B. Champagnon, "Density and concentration fluctuations in a erbium-doped fiber amplifiers glass: Raman and small angle X-ray scattering study," *J. Non-Cryst. Solids*, Vol. 351, 2421–2424, 2005.
13. Gómez, H. and M. de la L. Olvera, "Ga-doped ZnO thin films: Effect of deposition temperature, dopant concentration, and vacuum-thermal treatment on the electrical, optical, structural and morphological properties," *Mat. Sci. Eng.: B*, Vol. 134, 20–26, 2006.
14. Mazzali, C., D. C. Dini, E. Palange, and H. L. Fragnito, "Fast method for obtaining erbium-doped fibre intrinsic parameters," *Electron. Lett.*, Vol. 32, 921–922, 1996.
15. Zech, H., "Measurement technique for pump and signal background absorption of erbium doped fibers," *Electron. Lett.*, Vol. 31, 1866–1867, 1995.
16. Georges, T., "Comment on: Measurement technique for pump and signal background absorption of erbium doped fibres," *Electron. Lett.*, Vol. 32, 1126–1127, 1996.
17. Zech, H., "Reply to comment: Measurement technique for pump and signal background absorption of erbium doped fibres," *Electron. Lett.*, Vol. 32, 1127–1128, 1996.
18. Karimi, M. and F. E. Seraji, "Experimental technique for simultaneous measurement of absorption-, emission cross-section,

and background loss coefficient in doped optical fibers," *Appl. Phys. B: Lasers & Opt.*, Vol. 98, 113–117, 2010.

19. Karimi, M. and F. E. Seraji, "A novel method for simultaneous measurement of doped optical fiber parameters," *Eur. Phys. J. Appl. Phys.*, Vol. 50, 20701-6, 2010.
20. Karimi, M. and F. E. Seraji, "A proposed method to simultaneously measure doped optical fibers parameters," *Proc. Iran. Phys. Conf.*, 62–65, Kashan University, Iran, Jul. 15–18, 2009.
21. Karimi, M. and F. E. Seraji, "Theoretical performance analysis of doped optical fibers based on pseudo parameters," *Prog. Quant. Electron.*, 2010 (in press), doi:10.1016/j.pquantelec.2010.06.001.
22. Agrawal, G. P., *Fiber Optic Communication System*, 38, John Wiley & Sons, Inc., United Stated of America, 1992.
23. Ghatak, A. and K. Thyagarajan, *Introduction to Fiber Optics*, Cambridge University Press, 1998.
24. Desurvire, E., "Analysis of distributed erbium-doped fiber amplifiers with fiber background loss," *IEEE, Photon. Technol. Lett.*, Vol. 3, 625–628, 1991.
25. Giles, C. R. and E. Desurvire, "Modeling erbium-doped fiber amplifiers," *IEEE. J. Lightwave Technol.*, Vol. 9, 271–283, 1991.
26. Polyanin, A. D. and A. V. Mainchirov, *Hand Book of Mathematics for Engineers and Scientist*, Chapman & Hall/CRC Press, Taylor & Francis Group, Danvers, 2007.
27. www.stockeryale.com/o/fiber/products/edf-t10.htm, 2009.
28. www.pofc.com.tw/en/products/optical-fiber/specialty-fiber/rare-eaeth-doped-fiber/edf-c-band, 2008.